Spatial fluctuations in measures for spaciousness

Diemer de Vries, Edo M. Hulsebos, and Jan Baan
Laboratory of Acoustic Imaging and Sound Control, Department of Applied Physics, Faculty of Applied Sciences, Delft University of Technology, P. O. B. 5046, 2600 GA Delft, The Netherlands

(Received 31 May 2000; revised 13 March 2001; accepted 4 April 2001)

In room acoustics, several measures have been defined that are supposed to quantify the apparent source width (ASW) in a hall, being one of the perceptual cues related to spaciousness. The most common ones are the lateral energy fraction (LF), i.e., the ratio between lateral and omnidirectional early energy, and the interaural cross correlation coefficient (IACC), all to be calculated from measured or simulated impulse responses. [Several versions of the LF are known in literature, having different names, generalized here as lateral energy fraction.] According to a method proposed by Berkhout *et al.* [J. Acoust. Soc. Am. **102**, 2757–2770 (1997)], for a fixed source position impulse responses have been measured along an array of closely spaced microphone positions in several halls. The above measures, when calculated from these impulse responses, show large fluctuations with small variations in microphone position due to interference of the different components of the wave field to which the human ear is apparently insensitive. A revision of the measures is discussed, which contributes to the suppression of the interference effects. In order to assess their perceptual significance, the fluctuations have to be related to just-noticeable differences (jnd's) in ASW. Since very different jnd values are given in the literature, the authors advise that new experiments should be conducted on this point. © *2001 Acoustical Society of America.*
[DOI: 10.1121/1.1377634]

PACS numbers: 43.55.Gx, 43.55.Hy, 43.55.Br [JDQ]

I. INTRODUCTION

Many authors[1–7] have reported that the common room acoustics measures show significant variations with small spatial displacements of source or microphone. Bradley *et al.*,[1] and also Pelorson,[2] found that for all measures considered, in all halls investigated, a 30-cm displacement leads to significant variations. Nielsen *et al.*[4] find 1.4–3.2-dB differences for clarity index C80 values measured at eight points inside a single seat. Based on such results, most workers choose to determine the measures at numerous positions scattered over a hall, and calculate hall averages and standard deviations of the measures to describe the hall's acoustic quality. It then appears[2] that discrimination between halls with quite different geometrical characteristics—and probably quite different acoustic quality—is difficult and sometimes even not possible with these measures.

Apparent source width (ASW), together with envelopment determining the perception of spaciousness, is recognized as one of the most important subjective measures for estimating the acoustic quality of a concert hall or opera house. The interaural cross-correlation coefficient (IACC) and the lateral energy fraction (LF) have been devised as objective measures to quantify ASW. Recently, Okano *et al.*[6] determined specific versions of IACC and LF in several concert halls, including the Amsterdam Concertgebouw. They found that the variations in these measures over individual positions within one hall are of equal or larger order than the variations of average values between different halls.

In the publications referred to above, the measure variations are only described and discussed in a statistical way. This gives very little insight into the physical causes of these variations, except that it must have something to do with interference. Berkhout *et al.*[8] introduced multichannel array technology in room acoustical analysis: impulse responses are measured along a hall-wide closely spaced (0.05-m) array of microphone positions, along which one microphone is mechanically moved. It appears that observation of all measured responses in one display reveals their spatial coherence and gives ample insight into the wave structure of the sound field (see Fig. 3 of Ref. 8). Besides, calculation of room acoustic measures for each array position enables deterministic investigation of their spatial variations.

Okano *et al.* end their paper[6] with the remark that ''they welcome the results of further research on the strengths and weaknesses of LFs as an acoustic measure of real halls.'' Inspired by this quote, the authors decided to investigate, using array measurements and simulations, the spatial behavior of LF and also of the other ASW measures that Okano *et al.* discuss in their paper. The starting point was a multichannel response measured in the Amsterdam Concertgebouw.

II. OKANO *ET AL.*'s ASW MEASURES IN THE CONCERTGEBOUW

The authors measured 555 impulse responses in the Amsterdam Concertgebouw along an array of microphone positions with 0.05-m intervals over almost the full hall width (27.7 m), with an omnidirectional loudspeaker placed center-front stage. From all these impulse responses, the same ASW measures have been calculated as discussed by Okano *et al.*[6] First, there is the early lateral energy fraction LF_E as defined by Hidaka *et al.*[3] as

$$LF_E = \frac{\int_{0.005}^{0.080} p_8^2(t)\,dt}{\int_0^{0.080} p^2(t)} = \frac{\int_{0.005}^{0.080} p^2(t)\cos^2\phi\,dt}{\int_0^{0.080} p^2(t)}, \qquad (1)$$

where $p_8(t)$ is the sound pressure measured by a figure-8 microphone with the null axis pointed to the source, and $p(t)$ the sound pressure measured by an omnidirectional microphone at the same position. Note that the figure-8 microphone weighs the squared pressure—being a measure of sound energy—with $\cos^2\phi$, where ϕ is the azimuthal angle between the direction of incidence of a sound wave and the line through the microphone axis. The early lateral energy fraction as originally proposed by Barron and Marshall[9] contains a weighting factor $\cos\phi$ for the energy. For reasons of measurement simplicity, LF_E according to Eq. (1) is usually applied instead. Following Okano *et al.*, from each impulse response LF_E has been calculated for the octave bands of 125, 250, 500, and 1000 Hz, respectively. Also, the average of these four values (denoted by Okano *et al.* as LF_{E4}) has been determined, as well as the broadband value LF_{bb} calculated over the full four-octave signal bandwidth. [The authors measured the multichannel impulse response with a Soundfield SPS 422 microphone, which not only records the sound pressure, but also the three components of the particle velocity vector. This enables the synthesis of the figure-8 microphone necessary to calculate the numerator of LF_E during data processing.] Figure 1 shows the results as a function of microphone offset, i.e., the lateral coordinate with respect to the array center. It should be noted that one seat encompasses about ten data points. It is seen that, for the octave band values, the fluctuations show an almost-periodicity with offset, resembling an amplitude-modulated carrier wave. The ''carrier period'' decreases with frequency. In the band-averaged and broadband versions, this ''carrier wave look'' disappears.

The fluctuating behavior of the measures can be deterministically related to the wave field measured along the array. To this end, the first 80 ms *re* first arrival of each impulse response is Fourier transformed to the frequency domain. Figure 2 shows the ''acoustic fingerprint'' that results when the ''early amplitude spectra'' of all traces are displayed as a function of microphone offset. It is seen that for each frequency the data show a small-scale periodicity due to interference; the spatial wavelength slowly but monotonically decreases with increasing frequency, as expected. Within one octave band, the spatial wavelength variation is so small that the periodicity of the wave field, and of the energy-based acoustic measures derived from it, is maintained. When averaging over a broad frequency band, the fluctuations tend to cancel out.

The average values over the array do not strongly deviate from the hall-averaged values given in Ref. 6, Table III. Numerous seats can be found where the LF_E octave band values show fluctuations of about 0.15 around an average between 0.10 and 0.25. For the band-averaged and the broadband versions, the fluctuations per seat decrease to about 0.10 around averages between 0.20 and 0.30. For offsets around zero, fluctuations are much higher for all bands and bandwidths. This is to be expected, since in this area the strong specular side-wall reflections interfere. If one wants to avoid this area, one should place the microphone at least 2 m off the center line for the low-frequency bands, which is significantly less than the 5 m mentioned by Okano *et al.* For

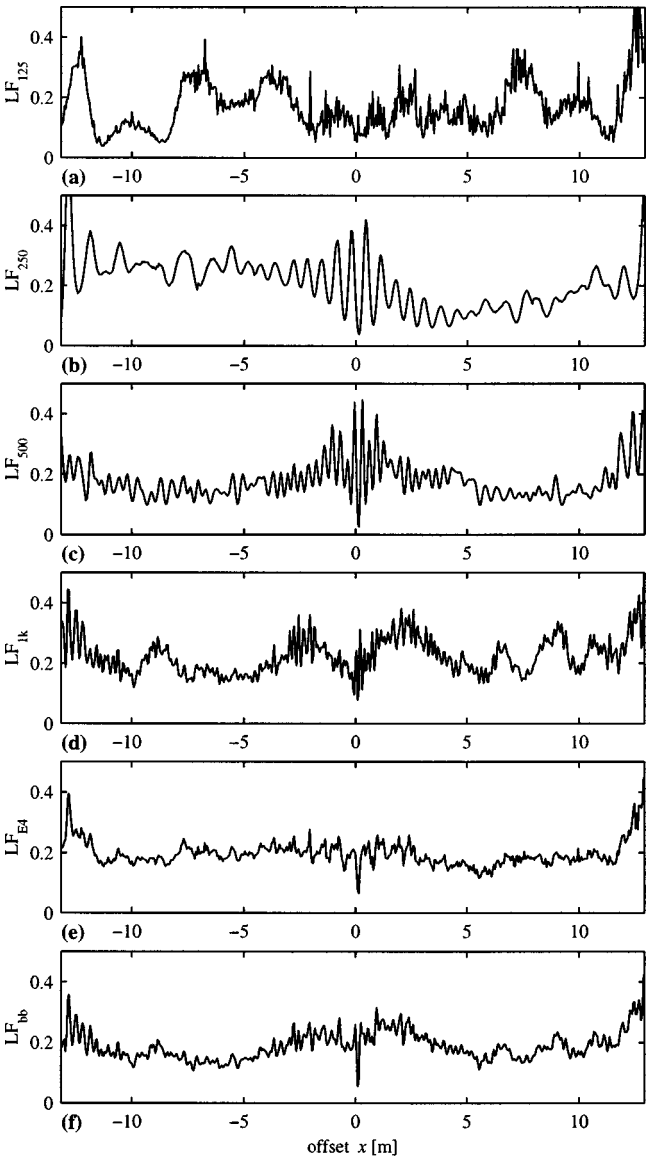

FIG. 1. Early lateral energy fractions calculated from the impulse responses measured in the Amsterdam Concertgebouw. From top to bottom, the values for the octave bands of 125, 250, 500, and 1000 Hz, the average value LF_{E4}, and the value for the full bandwidth are displayed as a function of microphone offset.

the band-averaged and the broadband versions, the behaviors of which show high similarity, an offset as small as 1 m is sufficient.

The second measure considered is the interaural cross-correlation coefficient IACC, introduced by Schroeder[10] and Ando[11] as the maximum within the delay time interval $|\tau| \leqslant 1$ ms of the crosscorrelation function $\rho_{lr}(\tau)$ between the pressures $p_l(t)$ and $p_r(t)$ at the left and right ear, respectively, of a real or dummy head, calculated over a time window $t_2 - t_1$

$$\rho_{lr}(\tau) = \frac{\int_{t_1}^{t_2} p_l(t)\, p_r(t+\tau)\, dt}{\sqrt{\int_{t_1}^{t_2} p_l^2(t)\, dt \int_{t_1}^{t_2} p_r^2(t)\, dt}}. \tag{2}$$

IACC has been calculated from binaural impulse responses measured with a KEMAR dummy head, being moved along the 555 array positions specified above. Fol-

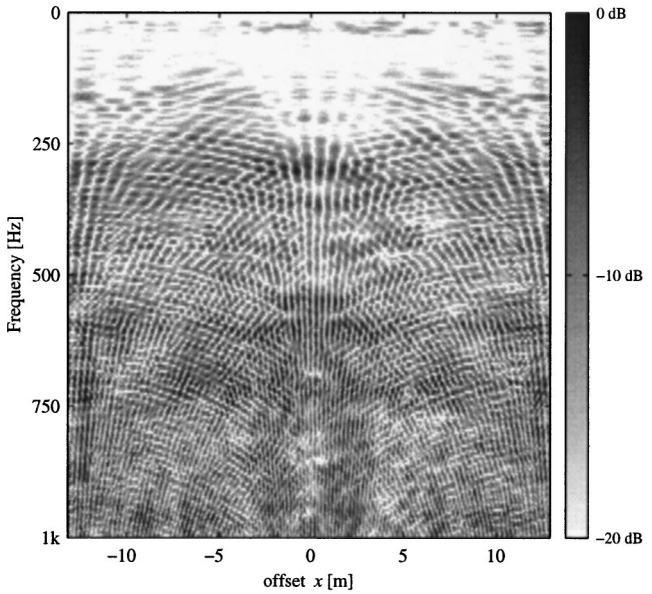

FIG. 2. The early amplitude spectra of the impulse responses measured in the Amsterdam Concertgebouw, obtained after Fourier transformation of the data between 0 and 80 ms *re* first arrival, as a function of microphone offset.

lowing again Okano *et al.*, the ''early'' 1-IACC between 0 and 80 ms (denoted by Okano *et al.* as 1-$IACC_E$) was calculated for the octave bands of 500, 1000, and 2000 Hz, respectively; the results are displayed as a function of dummy head offset in Fig. 3. Also, the average of the three octave band values is shown (denoted by Okano *et al.* as 1-$IACC_{E3}$), as well as the broadband version 1-$IACC_{bb}$ calculated over the full three-octave source bandwidth. As for LF_E, the values averaged over the array do not strongly deviate from the hall-averaged values given in Ref. 6, Table III. The fluctuations over a seat width are of the order 0.1, for all bands and bandwidths, around averages which strongly depend on frequency and bandwidth. As expected from the response pattern, also here the fluctuations are larger for the offsets around zero. To avoid this area, the microphone should be placed no less than 1 m off-center; this corresponds to the prescription given by Okano *et al.* There is a high similarity between the behavior of the band-averaged and the broadband version.

The results of this section confirm that there are large variations in the values of common measures for ASW, not only between seats in the same hall, but also at different positions at one and the same seat. [In deviation from the definition given in Eq. (1), the synthesized figure-8 microphone was always oriented in parallel with the array instead of with its null towards the source. This, however, does not affect the general conclusions following.] Octave band versions of LF_E and 1-$IACC_E$ fluctuate so strongly that their predictive value for ASW is highly questionable; band-averaged or broadband versions are preferred. But, the fluctuations in these versions also give rise to further questions. Given the fact that a listener in a concert hall will, in general, not perceive any change in ASW when he moves his head over a few centimeters, the difference limen in LF of 0.07, as indicated by Barron and Marshall[9] apparently does not hold in this situation. It seems that the measures considered are

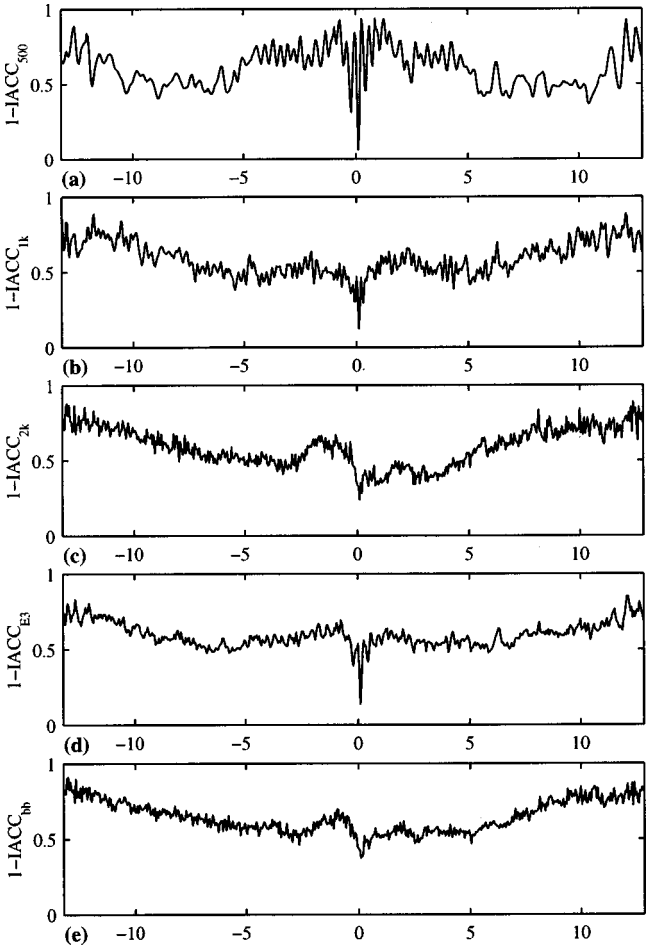

FIG. 3. 1-IACC calculated from binaural impulse responses measured in the Amsterdam Concertgebouw. From top to bottom, the values for the octave bands of 500, 1000, and 2000 Hz, the average value 1-$IACC_{E3}$, and the value for the full bandwidth are displayed as a function of dummy-head offset.

sensitive to local interference phenomena, where listeners are not, which suggests the formulation of new versions of these measures. This will be worked out in the following sections.

III. WEIGHTED BROADBAND VERSIONS OF ASW MEASURES

The strict time window boundary of 80 ms used in the early measures discussed above causes a discontinuity in the results: strong early reflections may suddenly disappear from the dataset when moving the microphone to the next array position. Therefore, in the following a smoothing time window $w(t)$ will be applied

$$w(t)=\begin{cases}1 & \text{for } 0<t<60 \text{ ms} \\ \cos^2 \pi(t-60)/80 & \text{for } 60<t<100 \text{ ms.}\end{cases} \tag{3}$$

In the previous section it was shown that determination of ASW measures after octave band filtering of impulse responses leads to large fluctuation of the resulting values. This fluctuation is smaller for broadband versions. Therefore, in the following only broadband measures will be considered, i.e., calculated over the full frequency range which is dominant for ASW perception. Potter *et al.*[12] showed that the dominant cues for spatial impression are found in the 500-Hz

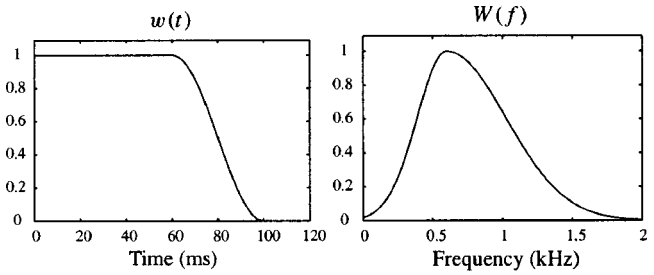

FIG. 4. Time and frequency windows applied to impulse responses when calculating ASW measures.

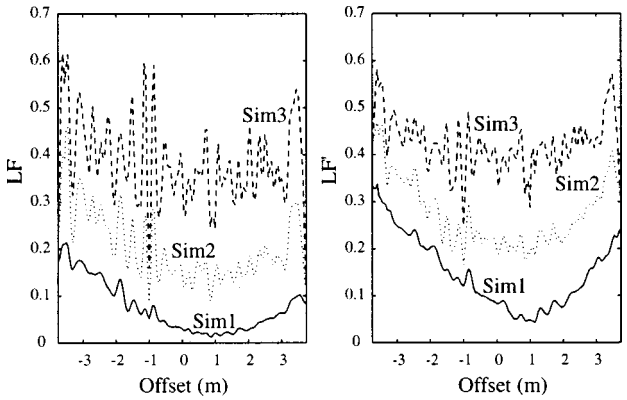

FIG. 5. LF and LF′ as a function of microphone offset, for sim1, sim2, and sim3.

octave band, corresponding with the dominance of frequencies around 600 Hz for lateralization earlier found by Raatgever[13] and specified by the following frequency window function:

$$W(f)=\begin{cases} e^{-(f/300-2)^2} & \text{for } f<600 \text{ Hz} \\ e^{-(f/600-1)^2} & \text{for } \geqslant 600 \text{ Hz}. \end{cases} \tag{4}$$

This window will be applied to all broadband measures treated in the remainder of this paper. Figure 4 depicts the two windows defined above. [When more low frequencies are included in the bandwidth, as suggested by Barron (Ref. 14), this will affect the fluctuating behavior of the measures. However, based on the results discussed in Sec. II, the order of fluctuation magnitude is expected to be the same.]

In order to discriminate the modified versions of the measures from those of Okano *et al.*, the subscript E will be dropped, although here the early part of the impulse responses is also considered. In further determinations of LF, the figure-8 microphone will be oriented, for each array position, with its null towards the source. Beside LF, the original version with the $\cos\phi$ weighting factor, to be denoted as LF′, will be calculated using velocity vector information. Also here, $\phi=\pi/2$ corresponds with the source direction for all array positions. Values of IACC are calculated from point simulations or measurements by applying a spatial filter based on the head-related transfer functions (HRTFs) of the KEMAR dummy head. This filter is described in the Appendix.

IV. SIMULATIONS AND MEASUREMENTS OF LF, LF′, AND 1-IACC

A. Simulations

Impulse responses were simulated for a rectangular room with dimensions $10\times7.5\times3$ m^3 using the mirror-image source model. The pressure reflection coefficient of front wall, rear wall (both 7.5×3 m^2), and floor is 0.8, that of the ceiling 0.5. The reflection coefficient of the left and right walls has been chosen as 0.2, 0.6, and 1.0 for the simulations sim1, sim2, and sim3, respectively. An omnidirectional source is positioned 3 m front, 1 m right, and 0.25 m below the room center. An array of pressure and velocity microphones with a 0.05-m spatial interval is situated 1.5 m above the floor, 2 m behind the room center over the full 7.5-m room width, thus encompassing 149 microphone positions. Figure 5 shows the values of LF and LF′ as a function of microphone offset. It is seen that for low side-wall reflectivity (sim1) the measures have low values, as expected. Local fluctuations are small in an absolute sense (<0.05), but relatively large (order 50%). Minimum values of the average curves are found for minimum distance between source and detector. From there, they monotonically increase towards the side walls. This can be understood as follows. When placed opposite the source, the synthesized figure-8 microphone has its sensitivity lobes perpendicular to the side walls, from which direction no specular reflections are incident: for the given configuration, the angle of incidence of the side-wall reflections on the array is about 45°. When moving towards the side walls, the figure-8 microphone facing the source with its null more and more turns its lobes into the directions of incidence of the reflections from the nearest side wall as well as from the front and rear walls. This yields an increase of the numerators of LF and LF′, whereas there is no argument in assuming that the common denominator shows this tendency as well. For increasing side-wall reflectivity (sim2, sim3), the average LF and LF′ curves shift upward, preserving their global shapes. The local fluctuations increase in an absolute sense (order 0.1 for sim2, order 0.2 for sim3), staying of order 50% in a relative sense.

Earlier, it had been stated that the fluctuations are caused by interference effects. This will now be considered in more detail. Figure 6(a) shows the offset-travel time representation of p and $p\cos\phi$ (the latter being proportional to the lateral velocity component) of two equal plane waves incident on the array under angles ϕ_0 and $\pi-\phi_0$, respectively—to be considered as an approximation of two reflections from opposite side walls—which cross each other at zero offset. Note that, due to the counterphase of the two lobes of the figure-8 microphone, $p\cos\phi$ has opposite sign for the two waves, yielding value zero at zero offset. Figure 6(b) shows offset-travel time representations of $p^2\cos^2\phi$ (the numerator integrand of LF), $p^2\cos\phi$ (the numerator integrand of LF′), and p^2 (the denominator integrand of both LF and LF′), together with their integrated values as a function of offset. It is seen that local minima of LF and LF′ are found at the interference point. In case of two waves in counterphase, local maxima are found. In general, it can be concluded that interference of waves gives rise to fluctuations.

The equivalent of Fig. 6(b) for the simulated wave field of sim2 is shown in Fig. 7. Again, interference of waves

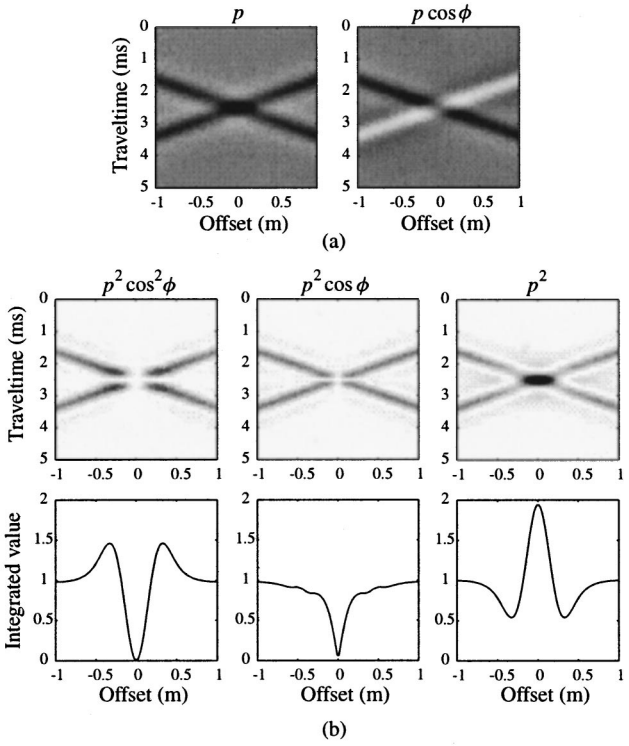

FIG. 6. (a) p and $p\cos\phi$ for two interfering identical plane waves, and (b) the offset-travel time representations of $p^2\cos^2\phi$, $p^2\cos\phi$, and p^2, together with their integrated values.

gives rise to strong fluctuations in both the numerators and the denominator of LF and LF′. Note that the numerator curves confirm the tendency of increase towards the side walls, in contrast to the denominator, which on the average remains constant.

Figure 8 shows the values of 1-IACC as a function of microphone offset for sim1, sim2, and sim3. The global

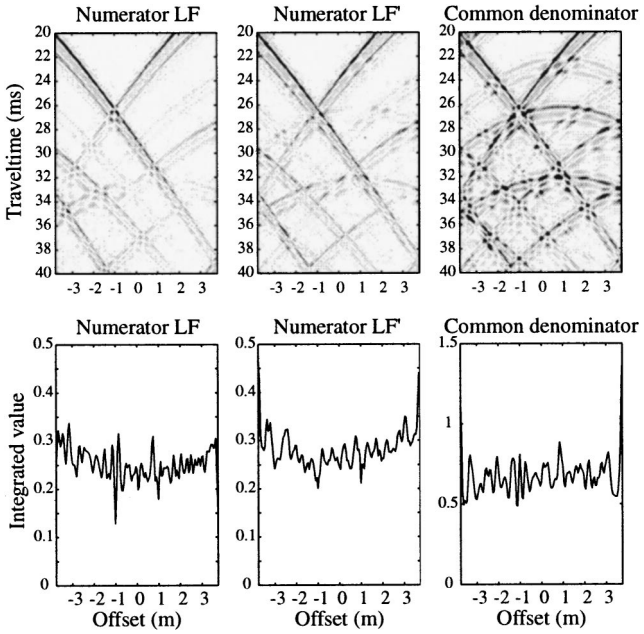

FIG. 7. Offset-travel time representations of the numerator integrands of LF and LF′ and their common denominator integrand, together with their integrated values.

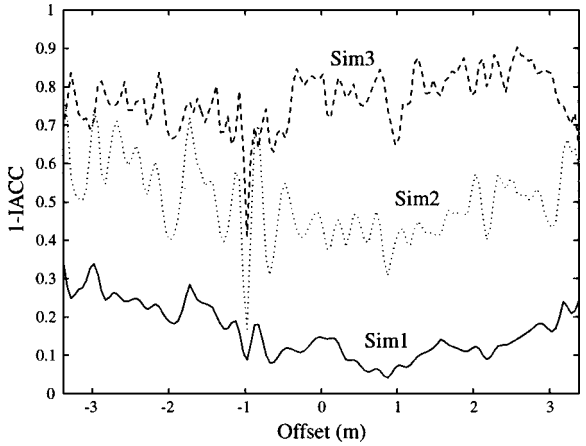

FIG. 8. 1-IACC as a function of microphone offset, for sim1, sim2, and sim3.

shapes of the curves are similar to those of LF and LF′; again, a global minimum is found (not convincingly in sim3) for minimum distance between source and microphone. When the dummy head faces the source, the signals at both ears are similar and thus the correlation is high. When moving towards the side walls, KEMAR increasingly shields and distorts the signal to the ear turned away from the source such that the interaural cross correlation decreases and 1-IACC increases. Also here, large local fluctuations occur, of the order 0.1 (50%) for sim1, 0.2 (40%) for sim2, and 0.2 (25%) for sim3. Here, the fluctuations decrease in a relative sense with increasing reflectivity. Since the numerator of the cross-correlation function [Eq. (2)], being a cross-energy density, has the same character as $p^2\cos\phi$, and the denominator is determined by two squared pressures, the fluctuations can be assigned to interference in a similar way as for LF and LF′.

B. Measurements

In the same way as earlier in the Amsterdam Concertgebouw, multichannel impulse response measurements have been done in the concert hall ''De Doelen'' in Rotterdam. The source was placed center-front stage, 12 m in front of an array of microphone positions over almost the full width (25 m) of the hall's main floor—a highly symmetric configuration. Figure 9 displays the values of LF and LF′ as a function of microphone offset. Here, the strong dip at zero offset is

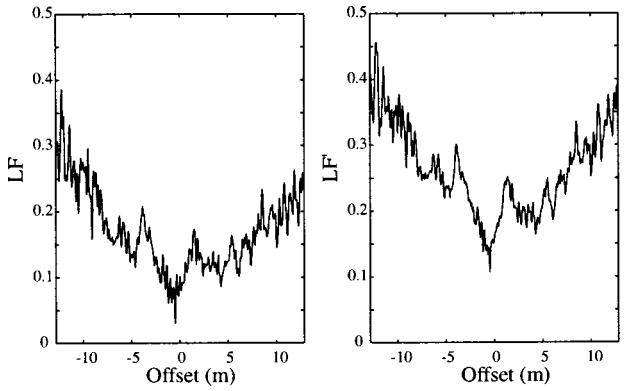

FIG. 9. LF and LF′ as a function of microphone offset, calculated from impulse responses measured in De Doelen, Rotterdam.

not so much caused by the synthesized figure-8 microphone looking perpendicular to the side walls—De Doelen has a hexagonal floorplan—as well by the strong interference between the two first-order side-wall reflections. Figure 10 shows the values of 1-IACC as a function of dummy-head offset. Again, the global shape is in good agreement with those of LF and LF′.

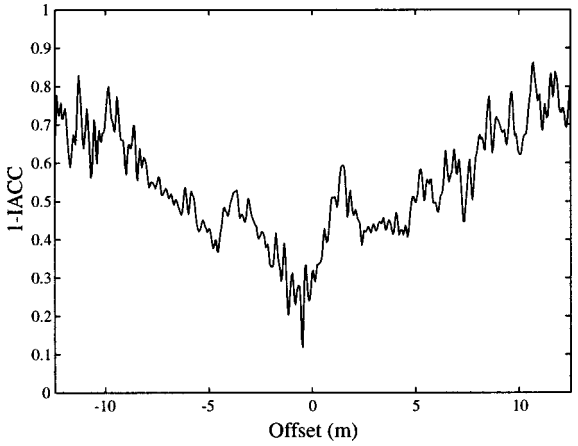

FIG. 10. 1-IACC as a function of dummy-head offset, calculated from impulse responses measured in De Doelen, Rotterdam.

V. THE LATERAL FRACTIONS REVISITED

In the previous section it was shown how the ASW measures fluctuate due to interference of wave-field components. Since ASW perception generally does not fluctuate correspondingly, it seems that the human auditory system is insensitive to these interference phenomena. Therefore, it is proposed to defined ASW measures of the same type as LF and LF′, but now based on the energies of the noninterfering wave-field components. This could be done by decomposing the wave field into plane waves by a double, i.e., temporal and spatial, Fourier transformation or a Radon transformation[8] of the offset-travel time dataset to the wave-number–frequency domain or the ray parameter–intercept time domain, respectively. This method, however, is not very accurate because of smearing effects due to the finite array length. Therefore, as an alternative method of decomposition, the wave field is separated by the nine spatial beam filters $\rho_n(x,t)$, $n=0,1,...,8$, as described in the Appendix. For each array microphone position x_m, the data are convolved in time with the corresponding trace $\rho_n(x_m,t)$ of the beam filter and the results are added for all microphone positions. Beam filter $\rho_0(x,t)$ is designed such that its directivity pattern $S0$ is given by

$$S0=\begin{cases}\cos(8\phi) & \text{for } -\pi/8<\phi<\pi/8\\ 0 & \text{for all other } \phi.\end{cases} \tag{5}$$

The other filters are chosen such that the corresponding directivity patterns are angle-shifted versions of $S0$, as illustrated in Fig. 11. A cosine shape has been chosen since in this case the sum of the squares of the overlapping filters equals 1 in all directions. This means that a mirror-image source gives the same contribution to the total energy as without beam filtering, but now without interference. For each beam, we calculate the lateral and the omnidirectional energy contributions and add these contributions to calculated the beam-filtered early lateral energy fractions BLF and BLF′ defined as

$$\mathrm{BLF}=\frac{\int_{0.005}^{0.080}\Sigma_{n=0}^{8}(\Sigma_m\rho_n(x_m,t)*p(x_m,t)\cos\phi)^2dt}{\int_{0.005}^{0.080}\Sigma_{n=0}^{8}(\Sigma_m\rho_n(x_m,t)*p(x_m,t))^2dt}, \tag{6a}$$

and

$$\mathrm{BLF}'=\frac{\int_{0.005}^{0.080}\Sigma_{n=0}^{8}(\Sigma_m|\rho_n(x_m,t)*p(x_m,t)\cos\phi||\rho_n(x_m,t)*p(x_m,t)|)dt}{\int_{0.005}^{0.080}\Sigma_{n=0}^{8}(\Sigma_m\rho_n(x_m,t)*p(x_m,t))^2dt}. \tag{6b}$$

The values of BLF and BLF′ as a function of microphone offset are given in Fig. 12, for the central parts of the simulated datasets sim1, sim2, and sim3, together with the values of LF and LF′ earlier shown in Fig. 5. It is seen that in the curves for the beam-split measure versions the strong local fluctuations are highly reduced, as expected. Figure 13 shows similar data for the impulse responses measured in De Doelen, with similar results.

VI. PERCEPTUAL RELEVANCE OF ASW MEASURE FLUCTUATIONS

Before the acoustical community decides to adopt new ASW measure versions, as proposed in the previous section, the perceptual relevance of the local fluctuations in the existing measures must be fully clarified. If it appears that these fluctuations do not correspond with perceptual differences—a result that is suggested by practical experience—and that the variations of the proposed new measures correspond with noticeable changes in ASW—which has to be investigated by new listening tests—it is worthwhile to consider the application of these new measures. Another smoothing operation is spatial averaging of the fluctuating values such that the ''carrier peridoicity'' is eliminated and the ''amplitude modulation'' remains. Again, the perceptual significance of the resulting variations has to be assessed by listening tests. A twofold conclusion can already be drawn: (1) the acoustic quality of a seat, or a group of neighboring seats, in terms of ASW cannot be quantified by one local measurement or calculation of the present measures LF, LF′, or IACC, which means that (2) there is no fixed local value of these measures that can form a criterion for ''good'' ASW.

In the literature, no unambiguous data on the percepti-

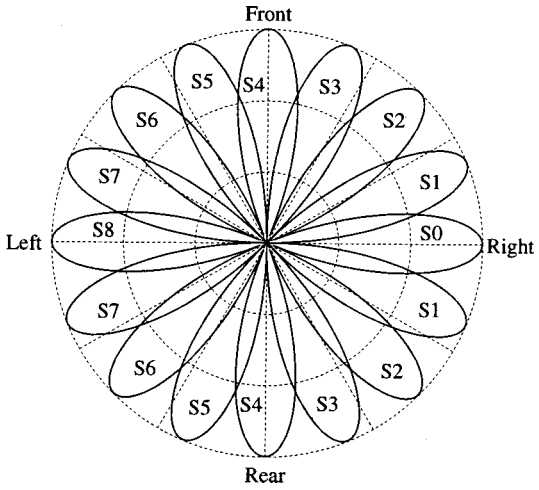

FIG. 11. Beam filters for plane-wave decomposition of multichannel impulse responses according to Eq. (5).

bility of ASW changes are found. Early results by Pollack *et al.*[15] on just-noticeable perceptual differences (jnd's) between binaural white-noise stimuli with different IACC values suggest that the jnd increases with decreasing IACC, just as the fluctuations in IACC reported in this paper. Based on the similar spatial behavior of LF, LF′, and 1-IACC, the jnd's for LF and LF′ are expected to increase with increasing values of the measures, just as the fluctuations in these measures. It is not certain that the jnd values found by Pollack *et al.* are also valid for musical signals heard in a concert hall, and that the noticed differences can be specified in terms of ASW. de Vries *et al.*[16] showed that, if this should be the case, the fluctuations hardly appear to be relevant from a perceptual point of view. However, using artificial impulse responses in an anechoic room convolved with music, Reichardt and Schmidt[17] found jnd's between 0.06 and 0.09 for LF′ varying from 0.2 to over 0.4; from a minimum value of LF′ around 0.3, the jnd increases for lower as well as higher LF′ values (Fig. 8 of Ref. 17). These jnd's are much lower then those estimated from the results of Pollack *et al.* (order 0.2 for LF′ around 0.3), but correspond with the difference limen of 0.07 that Barron[11] mentions. Cox *et al.*[18] find, for a simulated sound field in an anechoic room convolved with music, a jnd of 0.075 for IACC=0.33, which is much lower

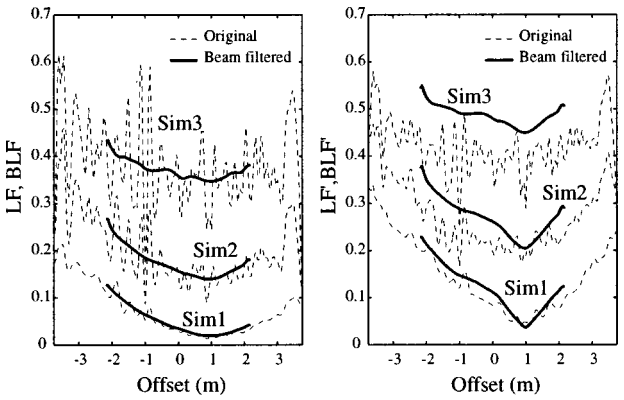

FIG. 12. LF and LF′ as a function of microphone offset for sim1, sim2, and sim3 (as in Fig. 5), together with their beam-filtered versions BLF and BLF′.

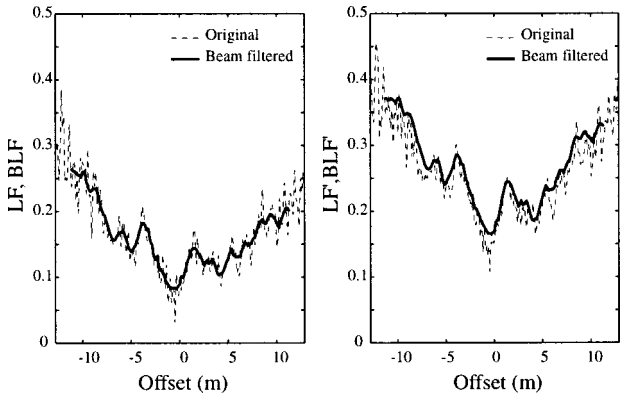

FIG. 13. LF and LF′ as a function of microphone offset calculated from impulse responses measured in De Doelen, Rotterdam (as in Fig. 9), together with their beam-filtered versions BLF and BLF′.

than the jnd of 0.38 indicated by Pollack *et al.* for the same IACC value.

Evidently, the question on the perceptual relevance of the fluctuations cannot be unambiguously answered using the literature data. New perceptual experiments should be carried out, preferably as a kind of ''round robin'' executed by institutes active in the field. The authors are readily prepared to make their array measurements available for this purpose.

VII. CONCLUSIONS

(i) Array measurements and simulations of impulse responses in halls reveal that the traditional ASW measures (LF, LF′, IACC) show large fluctuations on small spatial intervals (e.g., in front of one and the same seat) where no changes in ASW are perceived.

(ii) This means that a certain value of the traditional ASW measures does not correspond with a certain ASW; specification of ASW requirements in terms of local values of LF, LF′, or IACC is therefore useless.

(iii) Using the technique of beamforming, new versions of the existing ASW measures are proposed which—just as apparently the human auditory system—are insensitive to sound wave interference.

(iv) Based on the data from literature, the question of the perceptual relevance of the reported fluctuations cannot be unambiguously answered; new perceptual experiments should be carried out, preferably as a round robin.

APPENDIX: BEAM FILTERING

In order to reconstruct dummy-head measurements from microphone measurements (Sec. II), as well as for plane-wave decomposition of multichannel impulse responses (Sec. V), beam filters have been applied. The characteristics and the design of such filters are discussed in this Appendix.

Consider a linear array of M omnidirectional microphones at positions x_m $(m=1,...,M)$, a beam filter $\rho(x_m,t)$ and a pressure field $p(x_m,t)$ along the array. The output $z(t)$ of the beam filter is

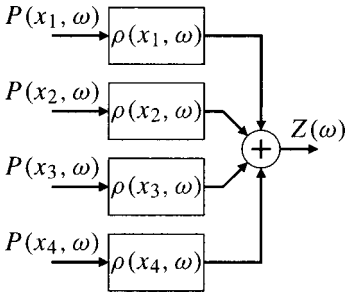

FIG. A1. Block diagram representation of Eq. (A2).

$$z(t)=\sum_{m=1}^{M}\rho(x_m,t)*p(x_m,t)$$

$$=\sum_{m=1}^{M}\int_{-\infty}^{\infty}\rho(x_m,t)p(x_m,t-\tau)d\tau. \tag{A1}$$

In practical situations only casual filters can be used, so that the lower limit of the integral in Eq. (A1) can be replaced by 0. In the frequency domain the convolution of Eq. (A1) becomes a multiplication

$$Z(\omega)=\sum_{m=1}^{M}\hat{\rho}(x_m,\omega)P(x_m,\omega). \tag{A2}$$

The output signal of a beam filter is thus obtained by filtering the signal at each microphone and adding all results, as illustrated in Fig. A1.

The directivity pattern of a beam filter $S(\omega,\phi)$ is defined as the response of the filter to plane waves with different angles of incidence. For the array of omnidirectional microphones considered here, the response only depends on the azimuth angle ϕ. In the frequency domain, the pressure along the array caused by a plane wave incident under this angle reads

$$P(x_m,\omega)=e^{j(\omega/c)x_m\cos\phi}. \tag{A3}$$

Substitution in Eq. (A2) yields for the directivity pattern

$$S(\omega,\phi)=\sum_{m=1}^{M}\rho(x_m,\omega)e^{j(\omega/c)x_m\cos\phi}. \tag{A4}$$

Note that the pattern is even in ϕ: waves incident on the array from front and rear under the same azimuthal angle cannot be discriminated.

A beam filter $\rho(x_m,t)$ that optimally approximates a specified directivity pattern can be designed by least-squares inversion, as shown in the following. The azimuthal angle is sampled as ϕ_n $(n=1,...,N)$. For each frequency component, Eq. (A4) can now be rewritten as a matrix equation

$$\mathbf{S}_n=\sum_{m=1}^{M}\mathbf{M}_{nm}\mathbf{P}_m, \tag{A5a}$$

with $\mathbf{S}_n=S(\omega,\phi)$, $\mathbf{P}_m=\hat{\rho}(x_m,\omega)$ and $\mathbf{M}_{nm}=e^{j(\omega/c)x_m\cos\phi}$, or in short

$$\mathbf{S}=\mathbf{MP}. \tag{A5b}$$

In order to obtain an optimal solution for $\mathbf{P}$ we apply a stabilized least-squares inversion to Eq. (A5b)

$$\mathbf{P}=(\mathbf{M}^*\mathbf{M}+c\mathbf{I})^{-1}\mathbf{M}^*\mathbf{S}, \tag{A6}$$

where c is a stabilization constant, $\mathbf{I}$ denotes the identity matrix, and $(.)^*$ means complex conjugation. Note that this inversion has to be carried out for each frequency component. For low values of c the matrix $\mathbf{M}^*\mathbf{M}+c\mathbf{I}$ becomes nearly singular and its inverse yields large eigenvalues, such that the filter may be very sensitive to noise. On the other hand, using a high value for c will result in a poor approximation of the desired directivity pattern. In general, the value $c=0.01$ yields a good compromise.

[1] J. S. Bradley and R. E. Halliwell, "Accuracy and reproducibility of auditorium acoustics measures," Proc. Inst. of Acoustics **10**, 399–406 (1988); J. S. Bradley, "Comparison of concert hall measurements of spatial impression," J. Acoust. Soc. Am. **96**, 3525–3535 (1994).

[2] X. Pelorson, J.-P. Vian, and J-D. Polack, "On the variability of room acoustical parameters: Reproducibility and statistical validity," Appl. Acoust. **37**, 175–198 (1992).

[3] T. Hidaka, L. L. Beranek, and T. Okano, "Interaural cross-correlation, lateral fraction, and low- and high-frequency sound levels as measures of acoustical quality in concert halls," J. Acoust. Soc. Am. **98**, 988–1007 (1995).

[4] J. L. Nielsen, M. M. Halstead, and A. H. Marshall, "On spatial validity of room acoustics measures," Proceedings of the 15th ICA Seattle, 2141–2142 (1998).

[5] K. Sekiguchi and T. Hanyu, "Study on acoustic index variations due to small changes in the observation point," Proceedings of the 15th ICA Seattle, 2121–2122 (1998).

[6] T. Okano, L. L. Beranek, and T. Hidaka, "Relations among interaural cross-correlation coefficient ($IACC_E$), lateral fraction (LF_E), and apparent source width (ASW) in concert halls," J. Acoust. Soc. Am. **104**, 255–265 (1988).

[7] D. de Vries and J. Baan, "Fluctuation of roomacoustical parameters on small spatial intervals," Collected Papers of the Forum Acusticum Berlin (CDROM), 5pAA3 (1999).

[8] A. J. Berkhout, D. de Vries and J. J. Sonke, "Array technology for acoustic wave field analysis in enclosures," J. Acoust. Soc. Am. **102**, 2757–2770 (1997).

[9] M. Barron and A. H. Marshall, "Spatial impression due to early lateral reflections in concert halls: The derivation of a physical measure," J. Sound Vib. **77**, 211–232 (1981).

[10] M. R. Schroeder, D. Gottlob, and K. F. Siebrasse, "Comparative study of European concert halls: Correlation of subjective preference with geometric and acoustic parameters," J. Acoust. Soc. Am. **56**, 1195–1201 (1974).

[11] Y. Ando, *Concert Hall Acoustics* (Springer, Berlin, 1985).

[12] J. M. Potter, F. A. Bilsen, and J. Raatgever, "Frequency dependence of spaciousness," Acta Acust. **3**, 417–427 (1995).

[13] J. Raatgever, "On the binaural proessing of stimuli with different interaural phase relations," Ph.D. thesis, Delft University of Technology (1980).

[14] M. Barron, "Measured early lateral energy fluctuations in concert halls and opera houses," J. Sound Vib. **232**, 79–100 (2000).

[15] J. Pollack and W. J. Trittipoe, "Binaural listening and interaural noise cross correlation," J. Acoust. Soc. Am. **31**, 1250–1252 (1959).

[16] D. de Vries, E. M. Hulsebos, and J. Baan, "Spatial fluctuation of spaciousness measures in auditoria," preprint 5147, 108th AES Convention (2000).

[17] W. Reichardt and W. Schmidt, "Die hörbaren Stufen des Raumeindruckes bei Musik," Acustica **17**, 175–179 (1966).

[18] T. J. Cox, W. J. Davies, and Y. W. Lam, "The sensitivity of listeners to early sound field changes in auditoria," Acustica **79**, 27–41 (1993).